

# On Spatial Domain Cognitive Radio Using Single-Radio Parasitic Antenna Arrays

D. Wilcox, *Member, IEEE*, E. Tsakalaki, *Member, IEEE*, A. Kortun, *Member, IEEE*,  
T. Ratnarajah, *Senior Member, IEEE*, C. B. Papadias, *Fellow, IEEE*, and M. Sellathurai, *Senior Member, IEEE*

**Abstract**—Spectrum sensing for cognitive radio is studied, using an electronically steerable parasitic antenna receptor (ESPAR), which relies on a single RF front end, and therefore meets the demanding low cost, power and size requirements of modern wireless terminals. We develop a strategy whereby the angular domain is divided into sectors, that are accessed via beamforming on a time division basis, to detect signals from primary users. We study the performance of detection metrics based on energy received per beam, and also eigenvalue-based detection statistics through considering the covariance matrix across the various directional beams. The ESPAR is able to achieve over 6dBi SNR improvement due to its beamforming capability. Further, once primary users' signals have been detected, directional transmit opportunities which do not interfere with active PUs become available, and we develop an adaptive beamforming algorithm to capitalise on these to efficiently utilise the spatial domain, which numerically optimises the beampattern and antenna efficiency using a convex formulation. The resulting beampatterns give between -20dB and -30dB nulls in the primary user direction.

**Index Terms**—Spectrum sensing, cognitive radio, ESPAR, parasitic antennas, smart antennas, eigenvalue-based sensing, energy detector, convex optimization

## I. INTRODUCTION

MODERN wireless communication networks have demanding design requirements impressed upon them. In particular, the requirement for energy efficiency is becoming progressively more important due to increasing energy costs and the environmental considerations of energy production, and this is foreseen as a trend which will continue. In addition, the data rate demand of network users is increasing and is projected to continue to do so [1]. On the other hand, the available electromagnetic spectrum for wireless communication is a finite resource, which must be used efficiently to achieve the requirements of future radio networks. A cognitive radio (CR) network is a communication system that has the ability to communicate more efficiently over the available spectrum by

detecting and utilizing unused spectrum [2]. Essentially, this requires the CR to perform sensing to detect licensed primary users (PUs), and make decisions as to whether spectrum holes exist, and therefore if transmit opportunities are available for transmission of data by secondary users (SUs). SUs should also prevent signal transmission which interferes with the PUs' communication, which is often specified as an upper bound on the allowed interference power to the primary network.

Accurate and low latency spectrum sensing is an essential part of the establishment of a cognitive radio network, but is practically challenging for several reasons. First, the signal to noise ratio (SNR) of the PU signal may be very low, for example, IEEE 802.22 requirements specify that wireless regional area network (WRAN) systems must be able to detect DTV signals at powers of -116 dBm with probability of detection equal to 0.9 and probability of false-alarm equal to 0.1. Second, there may be uncertainty about the noise power level at the receiver, which limits sensing performance [3]. Several general classes of spectrum sensing techniques have been developed, which each have various performance advantages depending on the sensing scenario [4]. For example, it is well known that for known signals in Gaussian noise, the matched filter maximises SNR and therefore detection probability [5]. However, often the receiver has to perform sensing with little or no information about the signal. On the other hand, blind sensing techniques such as energy detection [6] are simple and require no knowledge of the signal, but make assumptions about the noise power in the received signal, which is the main source of uncertainty. When multiple channels are available, eigenvalue-based sensing can be employed. Some eigenvalue test statistics are insensitive to uncertainties in noise [7], but the calculation of the test statistics can increase complexity in the receiver. Other sensing methods such as cyclostationary techniques [8] have been developed in the literature, but will not be considered in this work as we assume no knowledge of the signal characteristics.

While the majority of spectrum sensing work has considered multi-antenna systems where each antenna is connected to a separate radio-frequency (RF) receiver chain, in [9], [10] the authors consider spatial-domain spectrum sensing using an electronically steerable parasitic array receptor (ESPAR) [11]. Parasitic antenna technology uses a single RF chain to transmit and receive data, and as such is a practical solution to the constraints of size, weight, power and cost on a variety of radio equipment. Passive antennas which are mutually coupled to the active element allow analogue

D. Wilcox, A. Kortun and T. Ratnarajah are with the Institute for Digital Communications, The University of Edinburgh, The Kings Buildings, Mayfield Road, Edinburgh EH9 3JL, UK (e-mail: T.Ratnarajah@ieee.org).

E. Tsakalaki is with the Antennas, Propagation and Radio Networking (APNet) Section, Electronic Systems Department, Aalborg University.

C. B. Papadias is with the Athens Information Technology, Greece.

M. Sellathurai is with the Herriot-Watt University, Edinburgh Campus, Department of Electrical, Electronic and Computer Engineering, Edinburgh, EH14 4AS, UK.

Digital Object Identifier 10.1109/JSAC.2013.130321.

Manuscript received 15 April 2012; revised 18 September 2012. This work was supported by the Future and Emerging Technologies (FET) Programme within the Seventh Framework Programme for Research of the European Commission under FET-Open grant CROWN-233843.

beamforming which is achieved by varying tunable reactive loadings. This allows directional reception and transmission of data, and therefore *i*) provides a SNR gain for reception and transmission of directional signals, providing improved sensing and transmit/receive capability and *ii*) provides spatial filtering to mitigate in-band interference to and from PUs. Furthermore, the parasitic elements require mutual coupling to the active antenna, which *i*) requires closely spaced antenna elements which makes the antenna suitable for small mobile equipment applications, and *ii*) reduces the bandwidth of the antenna, limiting out-of-band interference to and from PUs. Parasitic antennas have also been shown to allow transmission of multiple data streams by projecting onto beamspace basis functions [12], [13].

In this work, we consider an ESPAR used as a cognitive radio transceiver, and in particular we investigate the accessing of the spatial domain for sensing, reception and transmission. On the sensing side, the approach we apply is to divide the spatial domain into sectors, which are accessed by directional beamforming on a time division basis from the parasitic antenna. This approach has been introduced in two previous works [9], [10] where aspects of space and frequency domain sensing using the ESPAR were introduced. In this work, we consider two approaches to sector-based sensing using the ESPAR. Firstly, we apply the energy detector to detect the presence of a directional signal within a particular sector. We also consider performance issues relating to the diversity i.e. the number of sectors used, between 1 sector (the omnidirectional antenna) and multiple sectors. Secondly, by oversampling the received signal at an appropriate rate, the signals from a PU received in each of the sectors will be correlated at each sample. Thus, the signal covariance matrix across the sectors will make eigenvalue-based sensing methods available to the receiver, and we compare the sensing performance of several eigenvalue-based metrics with the energy detector metric for ESPAR herein. In this manner, correlated signal energy from across different sectors can be combined to a single detection statistic, while maintaining a sense of directionality through the sector beamforming.

The advantages of sector-based sensing are twofold: firstly, the parasitic antenna enjoys a SNR gain from directional beamforming which will increase detection probability within that sector, thereby better protecting PUs from unwarranted SU transmissions; and second, directional information about the PU signals is automatically available from the sector sensing results. The benefit of having directional sensing information available is that the unoccupied spatial domain discovered through sector-based sensing represents directional transmit/receive opportunities which can be detected and utilised to increase spectral efficiency, whereas they would be missed if using an omnidirectional antenna. As such, in the second part of this work, we develop an efficient beamforming strategy to access the unused spatial domain for transmission and reception of SU signals using the parasitic antenna. Adaptive beamforming using parasitic antennas is challenging due to the lack of a closed form solution to the beampattern design problem for the tunable parasitic loads, and furthermore, the function is non-convex, so globally optimal solutions cannot be found efficiently [14]. The solution we propose iterates a

convex optimisation problem which uses a Euclidean distance metric to remain close to the feasible set of solutions, and simple projection operation.

The remainder of the paper is organised as follows. In section II, we present the modelling of the parasitic antenna and the spatial beam response. In section III, we develop the signal model of the wireless channel, and present the spectrum sensing metrics which will be applied to the parasitic antenna. In section IV, we show the simulated performance of the energy detector and eigenvalue-based metrics applied to the rotating switched beam parasitic antenna. In section V, we present the adaptive ESPAR beamforming algorithm to capitalise on available spatial domain transmit/receive opportunities with some examples of the resulting beampatterns and convergence properties, and we draw our conclusions from the work in section VI.

Notation: We denote scalars by non-bold lower and upper case,  $x$  and  $X$ , vectors by bold lower case,  $\mathbf{x}$  and matrices by upper case bold,  $\mathbf{X}$ .  $x^*$  denotes the complex conjugate,  $\mathbf{x}^T$  denotes the transpose operation, and  $\mathbf{x}^H$  denotes the conjugate transpose. Elements of the vector  $\mathbf{x}$  are denoted as  $\mathbf{x}(\cdot)$ , e.g. the first element as  $\mathbf{x}(1)$ . The operator  $|\cdot|$  returns the absolute value of the argument, while  $\text{diag}(\cdot)$  forms a diagonal matrix from the vector argument, and  $\mathcal{E}\{\cdot\}$  denotes the expectation operator.  $\mathbb{C}$  denotes the complex numbers,  $\mathbb{Z}$  denotes the set of integers, and  $j$  is the complex unit.

## II. ESPAR MODELLING

In this work, we consider an ESPAR receiver consisting of  $K + 1$  thin, half-wavelength dipoles. The ESPAR is a smart antenna system which has a significant advantage over its directional antenna counterparts, using only one active antenna and therefore requiring a single RF receive chain, but having the ability to control its antenna pattern as any smart antenna. In the design studied here, the passive elements (elements  $\{1 \dots K\}$ ) sit at equal angular separations on a circle of radius  $d$ , that is, the  $k^{\text{th}}$  antenna is located at angle  $\phi_k = (k - 1)\frac{2\pi}{K}$   $k \in \{1 \dots K\}$ , while the active element (element 0) is located at the centre of this circle. The antenna structure is shown in Fig. 1. Each of the passive elements is terminated through a reactive component, which can be tuned to alter the radiation pattern of the antenna as described below, while the active element feeds to a low noise amplifier which has an input impedance of  $Z_L$ . We use only reactive loadings as resistive components tend to reduce the efficiency of the antenna. In the following, we restrict our analysis to the 2-dimensional plane through the antenna, such that signal directions may be described by their azimuthal origin  $\phi$ , though the analysis can be easily extended to 3-dimensional signals. Let the  $k^{\text{th}}$  beampattern voltage response of the antenna which accesses the  $k^{\text{th}}$  angular sector be denoted as

$$B_k(\phi) = \mathbf{w}_k^T \mathbf{a}(\phi) \quad (1)$$

where  $\mathbf{a}(\phi)$  is the antenna manifold vector resulting from an incident plane wave originating from azimuth  $\phi$  which is defined from the array geometry as

$$\mathbf{a}(\phi) = [1 \ e^{-jd\frac{2\pi}{\lambda} \cos \phi} \dots e^{-jd\frac{2\pi}{\lambda} \cos \phi - (K-1)\frac{2\pi}{\lambda}}]^T \quad (2)$$

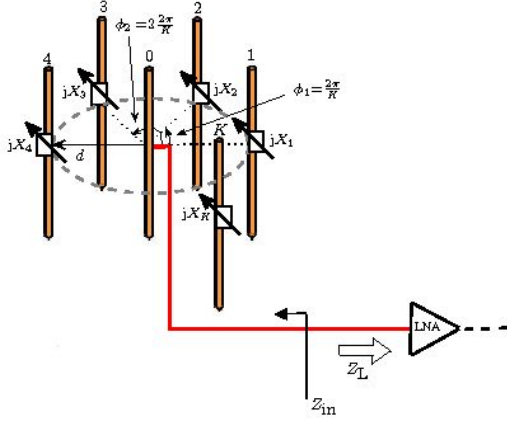


Fig. 1. Structure of example parasitic antenna receiver studied

where  $\lambda$  is the carrier wavelength. In (1),  $w_k$  is an equivalent weight vector for the  $k^{\text{th}}$  beampattern, defined as

$$w_k = Z_{L_k}^{-1} u \quad (3)$$

where  $u$  is a column selection vector (here,  $u = [1 \ 0 \ \dots \ 0]^T \in \mathbb{Z}^{(K+1) \times 1}$ ) and  $Z_{L_k} \in \mathbb{C}^{(K+1) \times (K+1)}$  is the loaded impedance matrix of the  $k^{\text{th}}$  beampattern:

$$Z_{L_k} = Z + X_k \quad (4)$$

The antenna mutual impedance matrix  $Z \in \mathbb{C}^{(K+1) \times (K+1)}$  can be calculated for an array of arbitrary elements through electromagnetic modeling software, or, for an array of half-wavelength thin electrical dipoles, using closed form equations, e.g. [15]. The matrix  $X_k$  is the  $(K+1) \times (K+1)$  diagonal matrix of the parasitic element reactances used to form the  $k^{\text{th}}$  beampattern, i.e.

$$X_k = \text{diag}([Z_L jx_k^T]) \quad (5)$$

where  $x_k$  is a vector of reactances which is designed to produce the desired beampattern for the  $k^{\text{th}}$  sector. Note that due to the topological symmetry of the antenna, each sector is illuminated by rotating the elements of  $x$  around the parasitic antenna elements, that is  $x_k$  is the  $(k-1)^{\text{th}}$  circular permutation of  $x$ , and so only a single value of  $x$  need be designed and stored. The optimised beampattern for the sector around  $0^\circ$  azimuth is shown in Fig. 2.

The active port impedance may be calculated as

$$Z_{\text{in},k} = \frac{1}{i_k(1)} u^T Z i_k \quad (6)$$

where  $i_k$  is the vector of currents induced in the antenna elements ( $i_k(1)$  is the first element thereof, relating to the active element) and is related to the equivalent weight vector by  $i_k = V_0 w_k$ , where  $V_0$  is the driving voltage in the active antenna. The efficiency of the antenna is calculated through the mismatch between  $Z_{\text{in},k}$  and  $Z_L$  as

$$\eta = 1 - \left| \frac{Z_{\text{in},k} - Z_L^*}{Z_{\text{in},k} + Z_L} \right|^2 \quad (7)$$

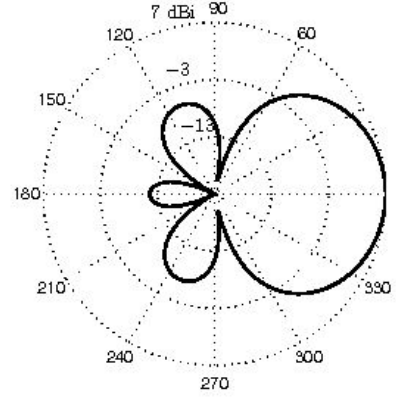


Fig. 2. Optimised beampattern for sector beamforming with maximum mainlobe gain

where we assume that the dipole antenna used has a radiation efficiency of 100%. Note that since  $x_k$  is a circular permutation of  $x$ , and the antenna topology has rotational symmetry of order  $K$ , the value of  $Z_{\text{in},k}$  remains constant  $\forall k$ , that is,  $Z_{\text{in},k} = Z_{\text{in}} \forall k$ . Therefore the matching efficiency  $\eta$  is maintained irrespective of the sector being accessed, which alleviates signal level mismatch between sectors.

### III. SIGNAL MODEL

In this section we present the signal modelling used to analyse the performance of the parasitic antenna. We divide the azimuthal plane into  $K$  sectors, with the  $k^{\text{th}}$  sector being centred on angle  $\phi_k = \frac{(k-1)}{K} 2\pi$ , such that the beampattern response of the  $k^{\text{th}}$  directional beampattern  $B_k(\phi)$  has its maximum at  $\phi_k$ . We model the impinging PU signal as having a power angular spread (PAS) denoted by  $A(\phi)$  which represents the probability density function (PDF) of the impinging wavefronts' angular distribution. The PAS can be parameterised by a mean angle of arrival AoA,  $\bar{\phi}$  and angular spread  $\sigma$ . For example, for a Laplacian PAS we have  $A(\phi) = \frac{c}{\sigma} e^{-\frac{|\phi - \bar{\phi}|}{\sigma}}$ , where  $c$  is a normalisation constant. Similarly, an isotropic PU signal distribution could be modelled through a uniform distribution. To calculate the gain of the antenna system in response to a PU signal, we calculate the distributed directivity gain of the  $k^{\text{th}}$  beampattern as:

$$G_k(\bar{\phi}) = \eta \frac{\int_0^{2\pi} B_k(\phi) B_k^*(\phi) A(\phi - \bar{\phi}) d\phi}{\frac{1}{2\pi} \int_0^{2\pi} B_k(\phi) B_k^*(\phi) d\phi} \quad (8)$$

During the sensing period, the ESPAR samples the angular domain with  $K$  spatial beams, and the received signals are written in a vector  $y = [y_1 \ \dots \ y_K]^T$ . Under the two hypotheses:  $\mathcal{H}_0$ , absence of primary signal(s); and  $\mathcal{H}_1$ , presence of primary signal(s), the baseband signal received in each spatial sector can be written as

$$\mathcal{H}_0 : y_k = n_k \quad (9)$$

$$\mathcal{H}_1 : y_k = r_k + n_k \quad (10)$$

where  $n_k$  is a noise term, and  $r_k$  is the PU signal(s) received at the ESPAR. Writing  $n = [n_1 \ \dots \ n_K]^T$  we have

$\mathbf{n} \sim \mathcal{CN}(\mathbf{0}, \sigma_n^2 \mathbf{I}_K)$ , i.e. the noise received in each sector beam has power  $\sigma_n^2$  and is uncorrelated across the spatial sampling. Note also that the noise  $\mathbf{n}$  is independent of the primary users' signals. Assuming there are  $P$  primary users transmitting independent signals, the PU signal received at the ESPAR in (10) can be expressed as

$$r_k = \sum_{p=1}^P h_p \sqrt{P_{T_p} G_k(\bar{\phi}_p)} s_p \quad (11)$$

where  $s_p$  is the signal from the  $p^{\text{th}}$  PU, transmitted with power  $P_{T_p}$ , and with a PAS with mean  $\bar{\phi}_p$ .  $h_p$  is the slow fading channel coefficient for the  $p^{\text{th}}$  PU signal, which also accounts for path loss in the signal model. Although we consider the slow fading model in this work, in a fast fading environment, each sample is modulated by a different channel gain. However, the long term performance is the same as the slow fading environment, as the samples have average channel gain  $\bar{h}_p$ . More importantly in this case is the sampling method, as the eigenvalue-based sensing methods require that the primary user samples ( $s_p$ ) are correlated for each sector, which may require a rotational sampling approach, depending on the symbol rate of the primary user. The receiver signal to noise ratio at the  $k^{\text{th}}$  beampattern (under hypothesis  $\mathcal{H}_1$ ) is

$$\gamma_k = \frac{1}{\sigma_n^2} \left( \sum_{p=1}^P |h_p|^2 P_{T_p} G_k(\bar{\phi}_p) \right) \quad (12)$$

where we have invoked the assumption that the signals originating from different PUs are uncorrelated. In the sequel, general SNRs are defined relative to an isotropic beampattern, for which  $G_{iso}(\bar{\phi}_p) = 1$ , and  $P_{T_p}$  can be calculated accordingly through (12).

There are two measures used to evaluate the sensing techniques, which are probability of detection ( $P_d$ ) and probability of false-alarm ( $P_{fa}$ ), defined as

$$P_{fa} = P(T > \kappa | \mathcal{H}_0) = \int_{\gamma}^{\infty} f_0(t) dt \quad (13)$$

$$P_d = P(T > \kappa | \mathcal{H}_1) = \int_{\gamma}^{\infty} f_1(t) dt, \quad (14)$$

where  $f_0(t)$  and  $f_1(t)$  are the PDFs of the test statistic  $T$  under the hypotheses  $\mathcal{H}_0$  and  $\mathcal{H}_1$ , respectively, and  $\kappa$  denotes the decision threshold.

In the following, we present the detection statistics and thresholds for the sector-based energy detector and eigenvalue-based detectors over the sector covariance matrix.

#### A. Energy Detector

The energy detector test statistic is formed from the squared value of the received signal in each beam integrated over the sample time,

$$T_{ED} = \int_0^T y_k(t)^2 dt \quad (15)$$

Under hypothesis  $\mathcal{H}_0$ , the decision statistic is the sum of the squares of  $N_S$  0-mean Gaussian distributed random variables with variance  $\sigma_n^2$ , thus  $T_{ED}$  will follow a central chi-square

distribution. Based on the cumulative distribution function (CDF) of  $T_{ED}$ , the probability of false alarm is given by [6]

$$P_{fa} = \Pr(T_{ED} > \kappa_{ED} | \mathcal{H}_0) = \frac{\Gamma\left(\frac{N_S}{2}, \frac{\kappa_{ED}}{2\sigma_n^2}\right)}{\Gamma\left(\frac{N_S}{2}\right)} \quad (16)$$

where  $\Gamma(\cdot)$  is the Gamma function and  $\Gamma(\cdot, \cdot)$  is the unregularised upper incomplete Gamma function [16]. Similarly, when a PU signal is present (i.e. under hypothesis  $\mathcal{H}_1$ ), the energy detector decision statistic has a chi-square distribution with a non-centrality parameter  $N_S \gamma_k$  [17], and we may statistically characterise the probability of detection over the  $k^{\text{th}}$  beampattern as

$$P_d = \Pr(T_{ED} > \kappa_{ED} | \mathcal{H}_1) = Q_{N_S/2} \left( \sqrt{N_S \gamma_k}, \sqrt{\frac{\kappa_{ED}}{\sigma_n^2}} \right) \quad (17)$$

where  $Q_z(\cdot, \cdot)$  is the generalized Marcum Q-function [16].

#### B. Eigenvalue-based Detection

The **statistical covariance matrix** of the cognitive user received signals over the  $K$  beampatterns can be written under the two hypotheses as

$$\mathbf{R}_{yy} = \mathcal{E}\{\mathbf{y}\mathbf{y}^H\} = \begin{cases} \sigma_n^2 \mathbf{I}_K & \mathcal{H}_0 \\ \mathbf{G} \mathbf{\Sigma} \mathbf{G}^H + \sigma_n^2 \mathbf{I}_K & \mathcal{H}_1 \end{cases} \quad (18)$$

where the  $(k, p)^{\text{th}}$  element of  $\mathbf{G} \in \mathbb{C}^{K \times P}$  contains  $h_p \sqrt{G_k(\bar{\phi}_p)}$  and  $\mathbf{\Sigma} \in \mathbb{R}^{P \times P}$  is a diagonal matrix with  $P_p$  on the  $p^{\text{th}}$  diagonal element. The diagonal elements of  $\mathbf{R}_{yy}$  give the energy received from each of the  $K$  beampatterns, i.e. an energy detector. The off-diagonal elements give a cross correlation between beams, which, assuming static channel conditions during the measurement period, will depend on the PAS of the PU signals impinging on the antenna, and the gain of the designed beampattern in other undesired sectors. Moreover, the eigenvalues,  $\lambda_{\max} = \lambda_1 > \dots > \lambda_K = \lambda_{\min}$ , of  $\mathbf{R}_{yy}$  under the  $\mathcal{H}_0$  are given by  $\lambda_i | \mathcal{H}_0 = \sigma_n^2 \forall i$ , and under the  $\mathcal{H}_1$  are given by

$$\lambda_i | \mathcal{H}_1 = \begin{cases} \sigma_i^2 + \sigma_n^2 & 1 \leq i \leq p \\ \sigma_n^2 & p < i \leq K \end{cases} \quad (19)$$

where  $\sigma_1^2, \dots, \sigma_p^2$  represent the received signal powers of the primary users. It is clear that the eigenvalues of the statistical covariance matrix  $\mathbf{R}_{yy}$  constitute a good test statistic to differentiate the two hypotheses  $\mathcal{H}_0$  and  $\mathcal{H}_1$ . However, we note that in order to apply eigenvalue-based metrics, the sample rate must be sufficient to capture correlated signals from each PU across each beampattern, i.e.  $K$  samples must be collected per symbol period of the PU. If this is not the case, the signal obtained from each beam,  $r_k$ , will be uncorrelated, and therefore  $\mathbf{R}_{yy}$  will be a diagonal matrix, and eigenvalue-based detectors will not be appropriate. The energy detector does not have this requirement on its sample-rate.

In that respect, the maximum eigenvalue detector uses the following test statistic

$$T_{MAX} = \lambda_{\max} \quad (20)$$

The test statistic  $T_{MAX} = \sigma_n^2$  under  $\mathcal{H}_0$  and  $T_{MAX} > \sigma_n^2$  under  $\mathcal{H}_1$ , therefore we have  $\kappa_{MAX} = \sigma_n^2$ . The maximum-minimum



eigenvalue (MME) detector uses the following test statistic

$$T_{MME} = \frac{\lambda_{\max}}{\lambda_{\min}} \quad (21)$$

The test statistic  $T_{MME} = 1$  under  $\mathcal{H}_0$  and  $T_{MME} > 1$  under  $\mathcal{H}_1$ , so we have  $\kappa_{MME} = 1$  [18]. The energy to minimum eigenvalue (EME) detector uses the following test statistic

$$T_{EME} = \frac{\sum \lambda_i}{\lambda_{\min}} \quad (22)$$

The test statistic  $T_{EME} = K$  under  $\mathcal{H}_0$  and  $T_{EME} > K$  under  $\mathcal{H}_1$ , so  $\kappa_{EME} = K$  [19]. In addition we use the generalized likelihood ratio test (GLRT) statistic, which is:

$$T_{GLRT} = \frac{\lambda_{\max}}{\sum \lambda_i} \quad (23)$$

The test statistic  $T_{GLRT} = \frac{1}{K}$  under  $\mathcal{H}_0$  and  $T_{GLRT} > \frac{1}{K}$  under  $\mathcal{H}_1$ , so we have  $\kappa_{GLRT} = \frac{1}{K}$  [20]. Notice that in the above thresholds,  $\kappa_{MAX}$  depends on knowledge of the noise variance, whereas the remaining eigenvalue based statistics are insensitive to fluctuations in the noise power due to their ratio forms.

Notice also that the above results represent ideal asymptotic thresholds for the infinite sample case. In practice we only have finite duration of sensing time to detect the primary user signals, hence we use sample covariance matrix to formulate the test statistic whereby the receiver collects  $N_S$  samples,  $\mathbf{y}_1 \dots \mathbf{y}_{N_S}$ . It should be noted that for the noise only case the sample covariance matrix of the received signal is going to be complex Wishart matrix, i.e., using a similar notation for the noise samples as to  $\mathbf{y}$  above

$$\hat{\mathbf{R}}_{nn} = \frac{1}{N_S} \sum_{i=1}^{N_S} \mathbf{n}_i \mathbf{n}_i^H \quad (24)$$

$$N_S \hat{\mathbf{R}}_{nn} = \mathbf{N} \mathbf{N}^H = \mathbf{W}, \quad (25)$$

where  $\mathbf{N} \sim \mathcal{CN}(\mathbf{0}, \sigma_n^2 \mathbf{I}_K \otimes \mathbf{I}_{N_S})$ ,  $\mathbf{W}$  is the complex central Wishart matrix and its distribution is denoted by  $\mathcal{CW}_K(N_S, \sigma_n^2 \mathbf{I}_K)$  [21]. From this noise only perspective i.e. under  $\mathcal{H}_0$ , and even for the finite sample case, exact thresholds for the detection problem based on the probability of false alarm can be developed, see for example [22], [23], [20]. Repetition of these expressions is omitted for brevity, and the interested reader is referred to the references above.

#### IV. ESPAR SPECTRUM SENSING PERFORMANCE

In this section we consider the sensing performance of a simulated parasitic antenna with  $K + 1$  half-wavelength thin electrical dipoles and antenna radial spacing  $d = \lambda/4$ . In the simulations results below, we use 10,000 random channel and noise realisations in a Monte-Carlo simulation environment. We also assume the input impedance of the LNA is matched to the ESPAR input impedance, i.e.  $Z_{in} = Z_L$ , so that the matching efficiency is 100%.

First, we consider the sensing performance of 2 ESPAR antennas, with  $K + 1 = 3$  and  $K + 1 = 7$ . For the 7-element ESPAR of thin half-wavelength electrical dipoles, the mutual impedance matrix  $\mathbf{Z}$ , (calculated using the analytical

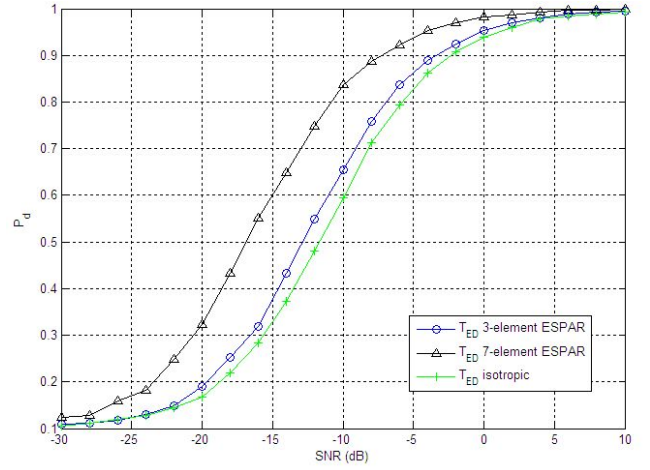


Fig. 3. Energy detector probability of detection through  $B_1(\phi)$  of the 3 and 7 element with  $P_{fa} = 0.1$

formulas of [15]) has the following form, due to symmetry and assuming reciprocity:

$$\mathbf{Z}^{[7]} = \begin{bmatrix} Z_{00} & Z_{01} & Z_{01} & Z_{01} & Z_{01} & Z_{01} & Z_{01} \\ Z_{01} & Z_{00} & Z_{01} & Z_{02} & Z_{03} & Z_{02} & Z_{01} \\ Z_{01} & Z_{01} & Z_{00} & Z_{01} & Z_{02} & Z_{03} & Z_{02} \\ Z_{01} & Z_{02} & Z_{01} & Z_{00} & Z_{01} & Z_{02} & Z_{03} \\ Z_{01} & Z_{03} & Z_{02} & Z_{01} & Z_{00} & Z_{01} & Z_{02} \\ Z_{01} & Z_{02} & Z_{03} & Z_{02} & Z_{01} & Z_{00} & Z_{01} \\ Z_{01} & Z_{01} & Z_{02} & Z_{03} & Z_{02} & Z_{01} & Z_{00} \end{bmatrix} \quad (26)$$

where  $Z_{00} = 73.07 + j42.5$ ,  $Z_{01} = 40.75 - j28.32$ ,  $Z_{02} = -0.66 - j35.93$ , and  $Z_{03} = -12.52 - j29.9$ . Similarly, for the 3 element ESPAR we have the mutual impedance matrix:

$$\mathbf{Z}^{[3]} = \begin{bmatrix} Z_{00} & Z_{01} & Z_{01} \\ Z_{01} & Z_{00} & Z_{03} \\ Z_{01} & Z_{03} & Z_{00} \end{bmatrix} \quad (27)$$

To realise the sector beamforming, the values in  $\mathbf{x}_k$  are optimised to maximise the average beamforming gain in the look direction  $\phi_k$ , via a constrained non-linear optimisation routine in MATLAB. **For the 3 element ESPAR, the optimised values are  $\mathbf{x}_1 = [92.4 \ 6.7]^T$  and  $Z_L = 90.2 - j97.6$ . For the 7 element ESPAR, the optimised values are  $\mathbf{x}_1 = [-33.4 - 160.780.7 - 160.1 - 33.2 - 71.9]^T$  and  $Z_L = 52.3 - j82.3$  giving 6.3dB maximum mainbeam gain.**

Assume there exists a single primary user, ( $P = 1$ ) which is modelled in the far field having PAS with mean at  $\bar{\phi}_1 = 0^\circ$  azimuth relative to the cognitive transceiver, and having angular spread  $\sigma_1 = 10^\circ$ . The detection performance through the first beampattern  $B_1(\phi)$  which is centred on  $0^\circ$  is shown in Fig. 3 for the 3 and 7 element ESPARs against a single isotropic antenna using the energy detector. The 7 element ESPAR has the best detection performance of the 3 antennas as its beamforming gain improves the receiver SNR, where the isotropic antenna has no beamforming gain, while the 3 element ESPAR performance falls between these two curves. Also, when the isotropic antenna detects the primary user it has no information about the directionality of this user, and therefore does not identify a transmit opportunity. The ESPAR antennas can then transmit and receive in the remaining

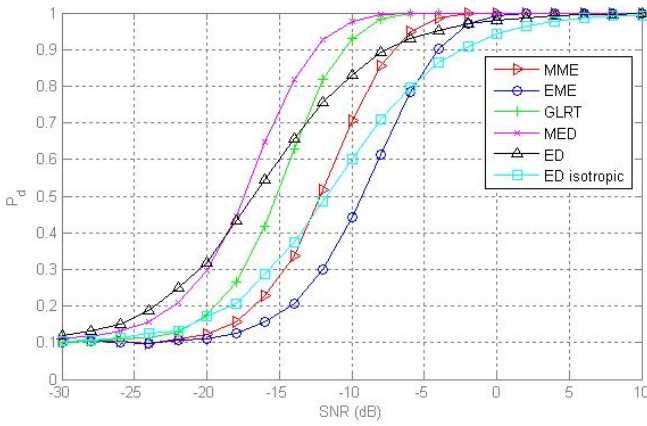



Fig. 4. Probability of detection using eigenvalue-based sensing metrics and energy detector.  $N_S = 10$  and  $P_{fa} = 0.1$

angular sectors, providing of course that these do not also contain primary users.

*Remark 1:* The antennas st perform spectrum sensing across the entire angular domain to identify transmit/receive opportunities. For the **isotropic antenna**, this requires only a single detection, but for the 3 and 7 element ESPARs, this requires 2 and 6 detection periods. Therefore the latency of the ESPAR sensing increases with  $K$ . However, it would be possible to form fewer beams from the 7 element ESPAR to sample the angular domain if lower latency was required.

*Remark 2:* The PU signal may have more or less angular spread than that used above, and the beampattern can be optimised for different levels of directionality, as the authors consider in [24]. In the limiting case of an isotropically impinging PU, the optimal beampattern is omnidirectional, and therefore directional sensing using ESPARs requires some PU directionality to improve sensing performance.

For the remainder of the paper, we consider the 7 element ESPAR only. In Fig. 4 we show the probability of detection over varying SNR for the energy detector (ED) and the eigenvalue-based metrics described in Section III. The same PU attributes of the previous example are used in this scenario. The energy detector metric is shown for the signal received through beampattern  $B_1(\phi)$  and also for an isotropic receiver. The maximum eigenvalue detector is shown to have the best performance, above the energy detector and GLRT statistics.

*Remark 3:* The eigenvalue-based statistics themselves do not give any indication of the directionality of the signal. However, the detection of the signal is improved over the single beam energy detector and therefore the PU is better protected against unwarranted transmissions using these methods. To capitalise on the directional transmit/receive opportunities, the sector covariance matrix  $R_{yy}$  can be reused. The diagonal elements of  $R_{yy}$  are themselves energy detectors for each sector, and can be used to determine which sector(s) contain the PU. Alternatively, subspace based methods such as the reactance domain MUSIC algorithm [25] could be used to accurately locate the PU.

The location of a PU is in general unknown to the cognitive user, and therefore there is no guarantee that the PU signal will be centred on the beam, i.e. the ESPAR will often suffer

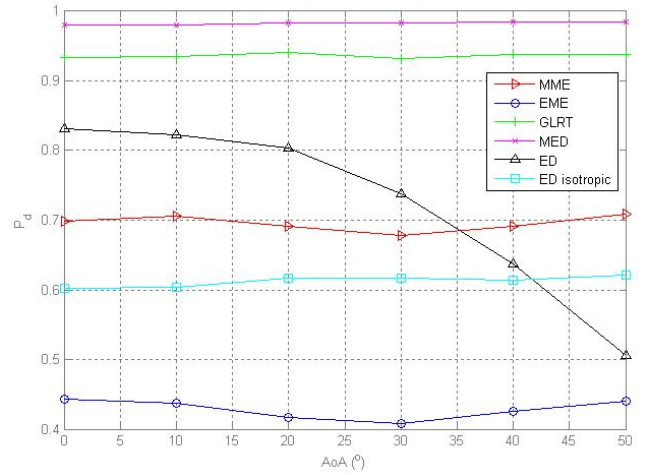


Fig. 5. Probability of detection using eigenvalue-based sensing metrics and energy detector for varying PU AoA. SNR=-10dB  $N_S = 10$  and  $P_{fa} = 0.1$

some beamshape loss. In Fig. 5 we show the probability of detection for the same performance metrics when the primary user is moved around the azimuthal plane. As the displacement angle increases, the performance of the energy detector is reduced due to beamshape loss. It is worth noting that above a displacement of  $30^\circ$  the second beampattern ( $B_2(\phi)$ ) would receive more energy from the primary user, and therefore this would offer the better detection probability. The eigenvalue-based test statistics do not suffer from beamshape loss due to the blind signal combination performed in the calculation of the test statistics, i.e. the signals from multiple sectors are combined to maintain the received signal power. The results above assumed perfect knowledge of the noise power. In reality, there will be some uncertainty about the noise level, i.e. the true noise power  $\sigma_{n(TRUE)}^2 = \alpha \sigma_n^2$ . In Fig. 6 we show the performance of the ESPAR using the GLRT, energy detector and maximum eigenvalue detectors with noise power uncertainty introduced. In this, we follow the approach of [26], where the value  $\beta = 10 \log_{10}(\alpha)$  and  $\beta$  is uniformly distributed over the interval  $[-b, b]$ , randomly generated on each Monte-Carlo run. The bound on the noise uncertainty,  $b$ , is varied from 0dB (perfect noise knowledge) to 2dB as shown in figure 6. This demonstrates that the energy detector and the maximum eigenvalue test statistics are **susceptible** to noise uncertainty, while the GLRT is not affected due to its ratio form which cancels any noise uncertainty parameter.

## V. ADAPTIVE BEAMPATTERN DESIGN FOR PARASITIC ANTENNAS

When directional spectrum holes are identified through spectrum sensing by the cognitive radio's parasitic antenna, it is necessary to utilise directional beampatterns which can capitalise on these available transmit opportunities. A simple approach would be to use a single available spatial channel using the same reactive loadings as the receiver sector beams. Alternatively, if multiple sectors are desired for transmission, pre-designed beampatterns which access these sectors could be accessed via a look-up table. A third approach would be to adaptively design a beampattern which accesses the desired

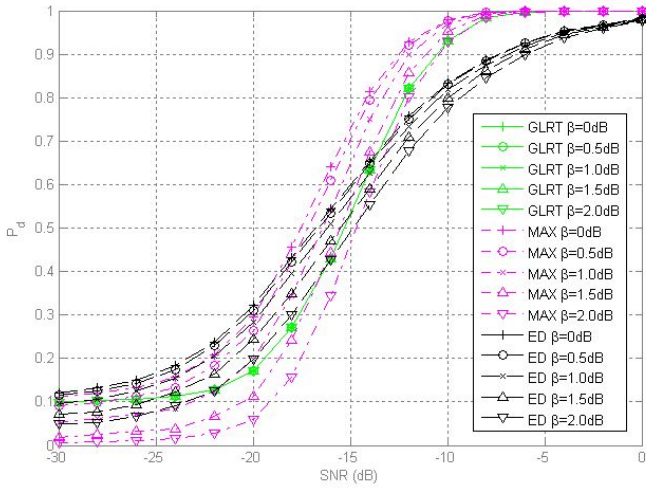


Fig. 6. Probability of detection using eigenvalue-based sensing metrics and energy detector with noise power uncertainty.  $N_S = 10$  and  $P_{fa} = 0.1$

angular domain, and in this section, we develop a design procedure for this purpose.

Beampatterns for parasitic antennas are commonly designed through exhaustive searches at the design stage and stored in a look-up table. It is possible to cancel the interference toward some desired geometrical directions by maximizing the cross-correlation coefficient between the desired and the realizable ESPAR beampatterns as described in [27]. Also, [28] [29] and [30] present numerical methods for SINR optimization and beam-null steering by maximizing the cross-correlation coefficient between a known reference (pilot) signal and the received signal. However, in these works, the matching efficiency of the antenna is not taken into account in the loading design, and also some of these methods would not be suitable for real-time applications such as sensing due to slow convergence. In this section, we develop a beampattern design strategy which iterates between a convex optimisation procedure and a simple projection operator, and also has the benefit of being able to take the matching efficiency into account in the loading design.

The design of beampatterns for parasitic antennas by varying the reactive loadings is a challenging problem. The beampattern is mathematically described in equation (1), where the equivalent weight vector  $\mathbf{w}$  varies with the inverse of the loaded mutual impedance matrix, as shown in equation (3). Closed form solutions to the design of  $\mathbf{w}$  that achieves a specified beampattern can be derived through a least squares approach, but they result in resistive loads which reduce antenna efficiency, or even negative resistances. There is no known closed form solution to the problem which gives zero real component in the parasitic loadings. Further, the problem is obviously not convex due to the inverse relationship of (3), so efficient numerical methods are not available.

Suppose we have  $N$  angular locations at which there is a beampattern null to be placed, and let  $\phi^{[N]} = [\phi_1 \dots \phi_N]^T$  be the vector of those angles. Similarly, we have  $D$  directions in which we desire a significant beampattern response, which are  $\phi^{[D]} = [\phi_1 \dots \phi_D]^T$ . Let  $\mathbf{A}(\phi) \in \mathbb{C}^{K+1 \times N}$  be a matrix whose columns are formed from steering vectors to these

null locations, i.e.  $\mathbf{A}^{[N]}(\phi) = [\mathbf{a}(\phi_1) \dots \mathbf{a}(\phi_N)]$ . Similarly, the matrix of steering vectors to the desired directions is  $\mathbf{A}^{[D]}(\phi) \in \mathbb{C}^{K+1 \times D}$ . To design the equivalent weight vector  $\mathbf{w}$  to achieve these beampattern constraints we solve:

$$\mathbf{w}^* = \arg \min_{\mathbf{w}} \mu_1 \|\mathbf{A}^{[N]T}(\phi)\mathbf{w}\|_2^2 + \mu_2 \|\mathbf{A}^{[D]T}(\phi)\mathbf{w} - \mathbf{b}\|_2^2 \quad (28)$$

where  $\mathbf{b} \in \mathbb{C}^{D \times 1}$  is a vector of desired beampattern magnitudes in the  $D$  directions in  $\phi$ , and  $\mu_1$  and  $\mu_2$  are weights on the importance of the nulls and desired direction magnitudes. Define  $\mathcal{L}$  as the set of values of  $\mathbf{w}$  such that  $\mathbf{X}$  (we drop the subscript used in section II previously to refer to the  $k^{\text{th}}$  beampattern) has the form given in (5). The inversion in equation (3) defines a non-linear one-to-one mapping between  $\mathbf{X}$  and  $\mathbf{w}$  (assuming  $\mathbf{Z}_L$  is non-singular), so that  $\mathcal{L}$  is a non-convex set, which cannot be traversed efficiently to guarantee a global solution. In general, the optimal value  $\mathbf{w}^* \notin \mathcal{L}$ , so it is necessary to approximate  $\mathbf{w}^*$  by a point in  $\mathcal{L}$ . Next, define  $\mathbb{P}_{\mathcal{L}}(\cdot)$  as a projection operator to the set  $\mathcal{L}$ . It is found that projecting  $\mathbf{w}^*$  directly onto  $\mathcal{L}$ , i.e.  $\tilde{\mathbf{w}} = \mathbb{P}_{\mathcal{L}}(\mathbf{w}^*)$  produces a poor approximation to the desired beampattern. However, due to the known relationships of (3) and (4), the feasible set can be constrained to be ‘close’ to  $\mathcal{L}$  around a given feasible point. Rearranging equations (3) and (4) we obtain

$$\mathbf{Z}\mathbf{w} + \mathbf{X}\mathbf{w} = \mathbf{u} \quad (29)$$

The first element of  $\mathbf{X}$  is the input impedance of the active antenna,  $Z_L$ , and therefore can be dealt with through a simple equality constraint (see (36) below). Given a proposed value of  $\mathbf{X} \in \mathcal{L}$ , and letting  $\tilde{\mathbf{Z}}_L$  be the matrix obtained by removing the first row of  $\mathbf{Z}_L$  we can remain close to the set  $\mathcal{L}$  around the feasible point by defined by  $\mathbf{X}$ , by maintaining the following Euclidean distance metric

$$\|\tilde{\mathbf{Z}}_L \mathbf{w}\|_2^2 < \delta \quad (30)$$

where  $\delta$  is some small constant. In this way, the projection  $\mathbb{P}_{\mathcal{L}}$  does not destroy the characteristics of the beampattern when applied to some designed value of  $\mathbf{w}$ , as  $\mathbf{w}$  lies within a small distance,  $\delta$ , of  $\mathcal{L}$ .

In addition, from equation (7) we see that the efficiency can be maximised by minimising the numerator of the fraction, i.e. the difference between  $Z_{in}$  and  $Z_L$ , and therefore this can be added as a further weighted second-order cone objective (see (34) below). The full optimisation problem for  $\mathbf{w}$  with the objectives and constraints described above is:

$$\mathbf{w}_i^* = \arg \min_{\mathbf{w}} \quad \beta^T \boldsymbol{\mu} \quad (31)$$

$$\text{subject to} \quad \|\mathbf{A}^{[N]T}(\phi)\mathbf{w}\|_2^2 < \mu(1) \quad (32)$$

$$\|\mathbf{A}^{[D]T}(\phi)\mathbf{w} - \mathbf{b}\|_2^2 < \mu(2) \quad (33)$$

$$\|[\mathbf{Z}\mathbf{w}](1) - Z_L \mathbf{w}(1)\|_2^2 < \mu(3) \quad (34)$$

$$\|\tilde{\mathbf{Z}}_L \mathbf{w}\|_2^2 < \delta \quad (35)$$

$$[\mathbf{Z}\mathbf{w}](1) + Z_L \mathbf{w}(1) - 1 = 0 \quad (36)$$

where  $\beta$  is an auxiliary vector, and  $\boldsymbol{\mu} = [\mu_1 \mu_2 \mu_3]^T$  contains the weights which define the Pareto-optimal solution. Notice that the objective is linear in  $\beta$ , while the constraints are either second-order cone constraints, or linear equalities in  $\mathbf{w}$ . Thus equations (31)-(36) form a convex optimisation problem.



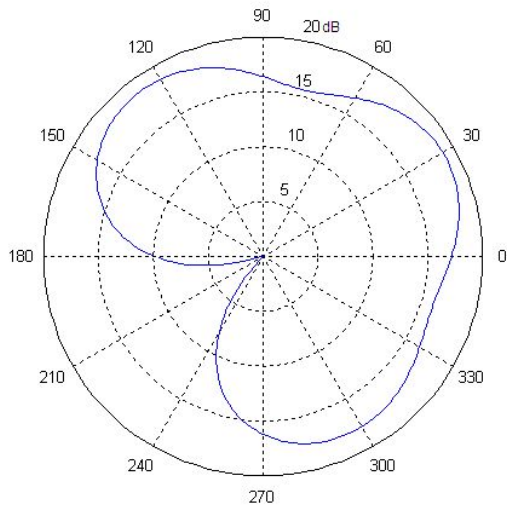


Fig. 7. Beampattern designed for 1 null at 210° azimuth. Null depth is around -30dB and efficiency is 86%

The iterative optimisation procedure progresses by selecting an initial value for  $\mathbf{X}_0$  and optimising over  $\mathbf{w}$  through problem (31) to obtain  $\mathbf{w}_1^*$ , from which a corresponding value  $\mathbf{X}_1^*$  can be obtained via closed form solution through equation (29). The projection of the solution  $\mathbb{P}_{\mathcal{L}}(\mathbf{w}_1^*)$  is achieved by setting real parts of  $\mathbf{X}_1^*$  to zero, apart from the first element which equals  $Z_L$  due to the constraint (36). At this point, the reactances can also be maintained within bounds on achievable values prescribed by hardware considerations. The vector  $\mathbf{w}$  is then re-optimised for the new value of  $\mathbf{X}$  and this procedure is iterated until convergence.

#### A. Beampattern Optimisation Performance

In this section we show some representative results of the algorithm's performance. The problem (31) was solved using the high-level modelling language YALMIP [31], and SeDuMi [32]. Fig. 7 shows the beampattern resulting from the design with 1 null at 210°. The null depth converges to -30dB below the peak beam response within 20 iterations and the efficiency reaches 86% after this time. **Figs. 8 and 9 show the convergence of the efficiency and the null depth respectively.** Fig. 10 shows the design of a beampattern with 2 nulls at 190° and 335°. These directions are effectively nulled, at -25dB and -31dB below the peak antenna response, which would effectively protect primary user terminals in these directions from interference. **Convergence results for this scenario are similar and so are not shown for brevity.** Finally, Fig. 11 shows the design with a sector nulled between 240° and 280°. This maintains below -20dB signal leakage to the sector containing the primary user. In the latter two examples, the design is more challenging due to the multiple nulls required, and the result is a drop in antenna matching. **In this case, some null depth can be traded-off for greater efficiency by varying the weighting vector  $\mu$ .**

## VI. CONCLUSION

We have shown that an ESPAR with a single active antenna can be used for directional sensing applications for cognitive

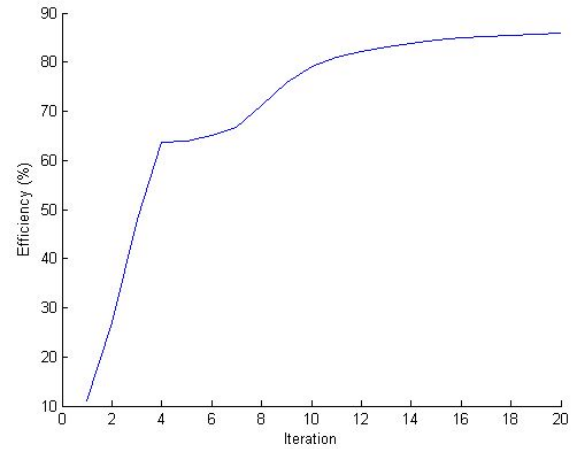


Fig. 8. Convergence of Antenna Efficiency for 1 null design

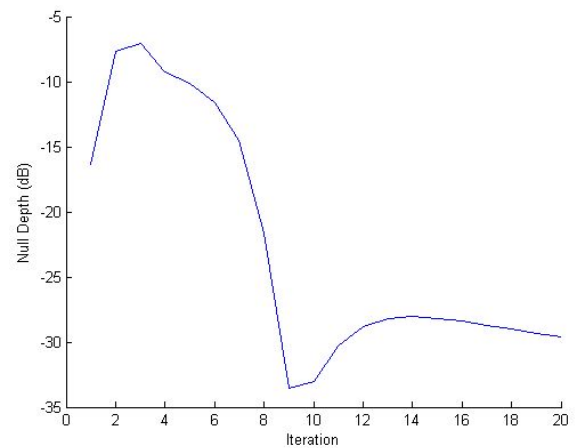


Fig. 9. Convergence of null depth for beampattern design with 1 null

radios. Sector beamforming both provides an SNR gain to give improved detection of PU signals (over 6dBi gain was achieved), and also provides spatial filtering which allows the ESPAR to locate directional PU signals, allowing for directional transmit/receive opportunities to be capitalised on by the cognitive transceiver. Several methods for detecting the presence of primary users have been addressed. The energy detector is a simple and effective method for detecting signal energy in each beam, but is susceptible to noise power uncertainty and also to the position of the primary user due to beamshape loss from the centre of the sector. Eigenvalue-based metrics can also be employed by forming the signal covariance matrix across the sector beams. This allows blind-combining of the incident primary signal in each sector, and therefore is insensitive to beamshape loss. The sampling requirements of the methods are different and lead to longer latency in the sensing for the directional methods. In the second section of the paper, we have demonstrated an adaptive beampattern design procedure used to create beampattern nulls which protects PUs from unwarranted transmissions by the cognitive radio, while allowing it to take full advantage of the unused spatial resources. The adaptive procedure also has the advantages that it takes into account antenna matching efficiency, while also



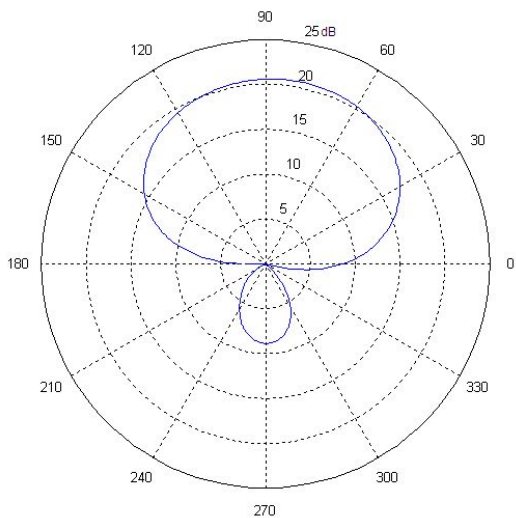


Fig. 10. Beam pattern designed for 2 nulls at  $190^\circ$  and  $335^\circ$  azimuth. Null depths are around -25dB and -31dB and efficiency is 69%

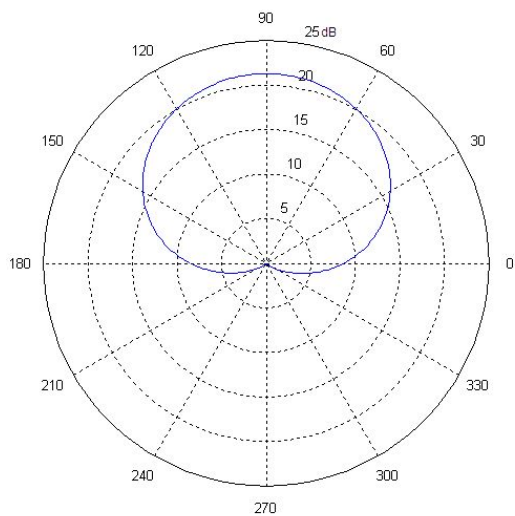


Fig. 11. Beam pattern designed for sector nulled between  $240^\circ$  and  $280^\circ$  azimuth. Null depth is -21dB and efficiency is 68%

benefiting from an efficient convex optimisation formulation and rapid convergence.

## REFERENCES

- [1] *Solving The Capacity Crunch: Options for Enhancing Data Capacity on Wireless Networks*, Onyeije Consulting LLC, 2011.
- [2] S. Haykin, "Cognitive Radio: Brain Empowered Wireless Communication," *IEEE J. Sel. Areas Commun.*, Vol. 23, pp. 201-220, Feb. 2005.
- [3] L. Shen, H. Wang, W. Zhang and Z. Zhao, "Blind Spectrum Sensing for Cognitive Radio Channels with Noise Uncertainty," *IEEE Trans. Wireless Commun.*, Vol. 10, pp. 1721-1724, June 2011.
- [4] T. Yucek and H. Arslan, "A Survey of Spectrum Sensing Algorithms for Cognitive Radio Applications," *IEEE Commun. Surveys Tutorials*, Vol. 11, pp. 116-130, Jan. 2009.
- [5] S. Kay, *Fundamentals of Statistical Signal Processing - Estimation Theory*, Prentice-Hall, 1993.
- [6] F. F. Digham and M-S. Alouin and M. K. Simon, "On the Energy Detection of Unknown Signals Over Fading Channels," *IEEE Trans. Commun.*, Vol. 55, pp. Jan. 2007.
- [7] Y. Zeng and Y. C. Liang, "Eigenvalue-based spectrum sensing algorithms for cognitive radio," *IEEE Trans. Commun.*, vol. 57, no. 6, pp. 1784-1793, 2009.
- [8] W. A. Gardner, Exploitation of Spectral Redundancy in Cyclostationary Signals, *IEEE Signal Processing Mag.*, Vol. 8, p. 1436, 1991.
- [9] E. P. Tsakalaki and O. N. Alrabadi and C. B. Papadias and R. Prasad, "Spatial spectrum sensing for wireless handheld terminals: Design challenges and novel solutions based on tunable parasitic antennas," *IEEE Wireless Commun. Mag.*, Vol. 17, pp. 33-40, Aug. 2010.
- [10] E. P. Tsakalaki and O. N. Alrabadi and C. B. Papadias and R. Prasad, "Spatial Spectrum Sensing for Cognitive Radios via Miniaturized parasitic Antenna Systems," In *Proc. Fifth International ICST Conference on Cognitive Radio Oriented Wireless Networks*, pp. 1-5, June 2010.
- [11] R. Harrington, "Reactively Controlled Directive Arrays," *IEEE Trans. Antennas Propag.*, Vol. 26, pp. 390-395, May 1978.
- [12] O. N. Alrabadi, J. Perruisseau-Carrier, A. Kalis, "MIMO Transmission Using a Single RF Source: Theory and Antenna Design," *IEEE Trans. Antennas Propag.*, Vol. , pp. 2011.
- [13] O. N. Alrabadi, C. B. Papadias, A. Kalis, R. Prasad, "A Universal Encoding Scheme for MIMO Transmission using a Single Active Element for PSK Modulation Schemes," *IEEE Trans. Wireless Commun.*, Vol. 8, pp. 5133-5142, Oct. 2009.
- [14] S. Boyd and L. Vandenberghe, *Convex Optimization* Cambridge University Press, 2004.
- [15] L. Petit, L. Dusopt, and J.-M. and Laheurte, "MEMS-Switched Parasitic-Antenna Array for Radiation Pattern Diversity," *IEEE Trans. Antennas Propag.*, Vol. 54, pp. 2624-2631, Sep. 2006.
- [16] L. Rade and B. Westergren, *Beta Mathematics Handbook*, Studentlitteratur, 2 ed., 1990.
- [17] F. F. Digham, M.-S. Alouini, and M. K. Simon, "On the energy detection of unknown signals over fading channels," In *Proc. IEEE International Conference on Communications*, Vol. 5, pp. 3575-3579, May 2003.
- [18] T. Ratnarajah, R. Vaillancourt and M. Alvo, "Eigenvalues and condition numbers of complex random matrices," *Society on Industrial and Applied Mathematics Journal on Matrix Analysis and Applications*, vol. 26, no. 2, pp. 441-456, January 2005.
- [19] C. Zhong, M. R. McKay, T. Ratnarajah, and Kai-Kit Wong, "Distribution of the Demmel condition number of complex Wishart matrices," *IEEE Trans. Commun.*, vol. 59, no. 5, pp. 1309-1320, May 2011.
- [20] A. Kortun, M. Sellathurai, T. Ratnarajah, and C. Zhong, "Distribution of the Ratio of the Largest Eigenvalue to the Trace of Complex Wishart Matrices," *IEEE Trans. Signal Process.*, Vol. 60, No 10, pp. 5527-5532, Oct. 2012.
- [21] T. Ratnarajah, "Spatially Correlated Multiple-Ananna Channel Capacity Distributions," *IEE Proc. Communications*, Vol. 153, No. 2, pp. 263-271, Apr. 2006.
- [22] A. Kortun, T. Ratnarajah, M. Sellathurai, C. Zhong and C. B. Papadias, "On the performance of eigenvalue-based cooperative spectrum sensing for cognitive radio," *IEEE J. Sel. Topics Signal Process.*, vol 5, no. 1, pp. 49-55, Feb. 2011.
- [23] T. Ratnarajah, C. Zhong, A. Kortun, M. Sellathurai and C. B. Papadias, "Complex random matrices and multiple-antenna spectrum sensing," *IEEE 36th Intern. Conf. on Acoustics, Speech and Sig. Process.*, May 2011.
- [24] E. P. Tsakalaki, D. Wilcox, E. Carvalho, C. B. Papadias, and T. Ratnarajah, Spectrum sensing using single-radio switched beam antenna systems, In *Proc. International ICST Conference on Cognitive Radio Oriented Wireless Networks*, June 2012.
- [25] C. Plapous, J. Cheng, E. Taillefer, A. Hirata, T. Ohira, "Reactance Domain MUSIC Algorithm for Electronically Steerable Parasitic Array Radiator", *IEEE Trans. Antennas Propag.*, Vol. 52, pp. 3257-3264, Dec. 2004.
- [26] Y. Zeng, Y-C Liang, E. Peh, and A. T. Hoang, "Cooperative Covariance and Eigenvalue Based Detections for Robust Sensing," In *Proc. Global Telecommunications Conference*, pp. 1-6, Dec. 2009.
- [27] E. P. Tsakalaki, O. N. Alrabadi, and C. B. Papadias, "Analogue Orthogonal Precoding using Reduced-Complexity Transceivers," In *Proc. IEEE International Symposium on Antennas and Propagation*, pp. 2845-2848, July 2011.
- [28] C. Sun, A. Hirata, T. Ohira, N. C. Karmakar, "Fast Beamforming of Electronically Steerable Parasitic Array Radiator Antennas: Theory and Experiment," *IEEE Trans. Antennas Propag.*, Vol. 52, pp. 1819-1832, July 2004.
- [29] Q. Han, V. Briand, and T. Ohira, "Evaluation of the Adaptive Beamforming Capability of an ESPAR Antenna Using the Genetic Algorithm," In *Proc. 9th European Conference on Wireless Technology*, pp. 59-62, Sep. 2006.
- [30] J. Cheng, Y. Kamiya, T. Ohira, "Adaptive beamforming of ESPAR antenna using sequential perturbation," In *Proc. IEEE MTT-S International Microwave Symposium Digest*, pp. 133-136, 2001.

- [31] J. Löfberg, "YALMIP : A Toolbox for Modeling and Optimization in MATLAB," *Proc. CACSD Conference*, <http://users.isy.liu.se/johanl/yalmip>, Taipei, Taiwan, 2004.
- [32] I. Polik, Sedumi 1.1 users guide. Available online: <http://sedumi.ie.lehigh.edu/>, 2005.



**David Wilcox** graduated from Cardiff University in 2006 with a BEng in Electronic Engineering. He received his PhD in Electronic Engineering from Queen's University Belfast in 2011. From 2010 to 2012, he was a Research Fellow at Queens University, where he worked on various R&D projects, both for DSTL and collaborative European projects. His research interests include radar, MIMO systems, estimation and optimisation theory. David has previously worked at QinetiQ, and currently works as an R&D Engineer at Camlin Technologies.



**Elpiniki Tsakalaki** is a postdoctoral fellow at the department of Electronic Systems, Aalborg University, Denmark, from where she received her Ph.D. in Wireless Communications in 2012. With a scholarship from the Hellenic Federation of Enterprises, she received in 2009 the M.Sc. in Information Networking from the Information Networking Institute, Carnegie Mellon University, with the highest honor. In 2008, she received the Diploma in Electrical and Computer Engineering from the National Technical University of Athens, Greece. In summer 2011, she

was an intern at the Nokia Siemens Networks Innovation Center, Spain, developing beamforming schemes for active base station antenna systems. Currently, she is working on the project "MIMO wireless communications for closely spaced antennas" granted by the Danish Council for Independent Research, Technology and Production Sciences. Her research interests are in the area of antenna design and signal processing including reconfigurable antenna arrays for diversity, MIMO systems and cognitive radio.



**Ayşe Kortun** received her B.Sc. and M.Sc. degrees in Electrical and Electronic Engineering from Eastern Mediterranean University, Cyprus in 2002 and 2004, respectively. She later worked as a lecturer at Cyprus International University in Cyprus. She received her Ph.D. degree in 2012 from the School of Electronics, Electrical Engineering and Computer Science at Queen's University Belfast, Belfast, U.K. Her current research interest is spectrum sensing techniques in cognitive radio wireless networks. Since January 2012 she has been working as a

Research Fellow at the Digital Communication Research Cluster at ECIT, Queen's University Belfast, Belfast, U.K.



**Tharmalingam Ratnarajah** (A96-M05-SM05) is currently with the Institute for Digital Communications, University of Edinburgh, Edinburgh, U.K., as a Reader in signal processing and communications. Since 1993, he has held various positions with the Queens University Belfast, Belfast, U.K., University of Ottawa, Ottawa, ON, Canada, Nortel Networks, Ottawa, ON, Canada, McMaster University, Hamilton, ON, Canada, and Imperial College, London, U.K. His research interests include random matrices theory, information theoretic aspects of MIMO

channels and ad hoc networks, wireless communications, signal processing for communication, statistical and array signal processing, biomedical signal processing, and quantum information theory. He has published over 175 publications in these areas and holds four U.S. patents. He is currently the coordinator of the FP7 Future and Emerging Technologies project HIATUS (2.7M) in the area of interference alignment and FP7 project HARP (3.2M) in the area of highly distributed MIMO. Previously, he was the coordinator of FP7 Future and Emerging Technologies project CROWN (2.3M) in the area of cognitive radio networks. Dr. Ratnarajah is a member of the American Mathematical Society and Information Theory Society.



**Constantinos B. Papadias** (SM03) received the Diploma of electrical engineering from the National Technical University of Athens (NTUA) in 1991 and the Doctorate degree in signal processing (highest honors) from the Ecole Nationale Supérieure des Télécommunications (ENST), Paris, France, in 1995. He is currently a Professor at Athens Information Technology (AIT), Athens, Greece, as well as the Academic Director of AIT's Doctoral Program, which runs in cooperation with Aalborg University, Aalborg, Denmark. He was a Researcher at Institut

Eucom, Stanford University, and Bell Labs, and was an Adjunct Professor at Columbia University and Carnegie Mellon University. His research interests span several areas of advanced communications systems, with emphasis on wireless, cognitive, green and next generation networks. He has published over 130 papers, five book chapters, one edited book, and has received over 3000 citations for his work. His distinctions include the 2002 Bell Labs Presidents Award, a Bell Labs Teamwork Award, the 2003 IEEE Signal Processing Society's Young Author Best Paper Award and ESI's most cited paper of the decade citation in the area of wireless networks in 2006. He has also made standards contributions (most notably as the coinventor of the Space-Time Spreading (STS) technique that was adopted by the cdma2000 wireless standard for voice transmission) and holds 12 patents. He is currently the Technical Coordinator of three EU FP7 research projects: CROWN, in the area of cognitive radio systems, HIATUS, in the area of interference alignment and HARP in the area of highly distributed MIMO. He is a coauthor of the book MIMO Communication for Cellular Networks which was recently published by Springer-Verlag.



**Mathini Sellathurai** received the Technical Licentiate degree from the Royal Institute of Technology, Stockholm, Sweden, in 1997 and the Ph.D. degree from the McMaster University, Canada, in 2001. She is currently a reader with Herriot-Watt University Edinburgh, U.K. Her current research interests include adaptive and statistical signal processing, space-time and MIMO communications theory, network coding, information theory and cognitive radio. Dr. Sellathurai was the recipient of the Natural Sciences and Engineering Research Council of Canada's

doctoral award for her Ph.D. dissertation and a co-recipient of the IEEE Communication Society 2005 Fred W. Ellersick Best Paper Award. Dr. Sellathurai is currently serving as an Associate Editor for the IEEE Transactions on Signal Processing.